© 2025 Journal of Pharmacy & Pharmacognosy Research, 13 (2), 647-661, 2025
ISSN 0719-4250
https://jppres.com

DOI: https://doi.org/10.56499/jppres24.2050_13.2.647

Original Article

Antidiabetic potential of isolated compounds from *Cyperus sexangularis* Nees: An *in silico* molecular docking and dynamic-based approach

[Potencial antidiabético de compuestos aislados de *Cyperus sexangularis* Nees: Un enfoque basado en la dinámica y el acoplamiento molecular *in silico*]

Gugulethu M. Miya[1], Pallab Kar[2*], Ayodeji O. Oriola[1*], Adebola O. Oyedeji[1,2*]

[1]Department of Chemical and Physical Sciences, Walter Sisulu University, Nelson Mandela Drive, P/Bag X1, Mthatha 5117, South Africa.
[2]African Medicinal Flora and Fauna Research Niche, Walter Sisulu University, Nelson Mandela Drive, P/Bag X1, Mthatha 5117, South Africa.
*E-mail: pkar@wsu.ac.za; aoriola@wsu.ac.za; aoyedeji@wsu.ac.za

Abstract

Context: Diabetes is a metabolic and chronic inflammatory disease that affects over 537 million people worldwide, with a projected rise to 783 million cases by 2045 if not put in check. Plant-derived compounds have continued to show strong anti-hyperglycemic activities with minimal adverse effects, with many more to be explored.

Aims: To estimate the potential therapeutic tendencies of the phytochemicals isolated from the leaf extracts of *Cyperus sexangularis* against α-amylase and α-glucosidase proteins implicated in hyperglycemia.

Methods: *In silico* molecular docking, drug-likeness profiling, and molecular dynamics (MD) studies.

Results: The isolated compounds were characterized by spectroscopic means to be dodecanoic acid, ethyl nonadecanoate, ethyl stearate, β-sitosterol, and stigmasterol. The interaction of stigmasterol with the α-amylase and α-glucosidase protein displayed the binding energy score of -10.0 kcal/mol and -7.6 kcal/mol, respectively. However, the standard antidiabetic drug (acarbose) exhibited a binding energy score of -8.6 and -4.6 kcal/mol. The physicochemical characteristics of the compounds by Lipinski's rule of five and Veber's rule suggested stigmasterol and β-sitosterol as promising compounds that can further be explored against diabetes. Furthermore, at 120 ns MD simulations, the RMSD and RMSF analysis of stigmasterol-α-amylase (1), β-sitosterol-α-amylase (2), stigmasterol-α-glucosidase (3) and β-sitosterol-α-glucosidase (4) complexes showed the fewest fluctuations, indicating the conformational stability of the respective complexes.

Conclusions: Identified bioactive compounds in *C. sexangularis* leaf extracts, notably stigmasterol and β-sitosterol, are the best-scoring lead compounds with remarkable inhibitory properties against α-amylase and α-glucosidase digestive enzymes implicated in diabetes.

Keywords: *Cyperus sexangularis*; diabetes; *in silico* molecular docking; molecular dynamics; stigmasterol; α-amylase and α-glucosidase enzymes.

Resumen

Contexto: La diabetes es una enfermedad inflamatoria crónica y metabólica que afecta a más de 537 millones de personas en todo el mundo, con un aumento proyectado a 783 millones de casos para 2045 si no se controla. Los compuestos derivados de plantas han seguido mostrando fuertes actividades antihiperglucémicas con efectos adversos mínimos, y hay muchos más por explorar.

Objetivos: Estimar las posibles tendencias terapéuticas de los fitoquímicos aislados de los extractos de hojas de *Cyperus sexangularis* contra las proteínas α-amilasa y α-glucosidasa implicadas en la hiperglucemia.

Métodos: Estudios *in silico* de acoplamiento molecular, perfil de similitud con fármacos y dinámica molecular (MD).

Resultados: Los compuestos aislados se caracterizaron por medios espectroscópicos como ácido dodecanoico, nonadecanoato de etilo, estearato de etilo, β-sitosterol y estigmasterol. La interacción del estigmasterol con las proteínas α-amilasa y α-glucosidasa mostró una energía de enlace de -10,0 kcal/mol y -7,6 kcal/mol, respectivamente. Sin embargo, el fármaco antidiabético estándar (acarbosa) mostró una energía de enlace de -8,6 y -4,6 kcal/mol. Las características fisicoquímicas de los compuestos según la regla de cinco de Lipinski y la regla de Veber sugirieron que el estigmasterol y el β-sitosterol son compuestos prometedores que pueden explorarse más a fondo contra la diabetes. Además, en simulaciones de MD de 120 ns, el análisis RMSD y RMSF de los complejos estigmasterol-α-amilasa (1), β-sitosterol-α-amilasa (2), estigmasterol-α-glucosidasa (3) y β-sitosterol-α-glucosidasa (4) mostraron las menores fluctuaciones, lo que indica la estabilidad conformacional de los respectivos complejos.

Conclusiones: Los compuestos bioactivos previamente identificados en los extractos de hojas de *C. sexangularis*, en particular el estigmasterol y el β-sitosterol, son los compuestos principales con mejor puntuación y con notables propiedades inhibidoras contra las enzimas digestivas α-amilasa y α-glucosidasa implicadas en la diabetes.

Palabras Clave: acoplamiento molecular *in silico*; *Cyperus sexangularis*; diabetes; dinámica molecular; estigmasterol; enzimas α-amilasa y α-glucosidasa.

ARTICLE INFO
Received: April 10, 2024.
Accepted: November 8, 2024.
Available Online: November 26, 2024.

AUTHOR INFO
ORCID:
0000-0002-3314-5391 (GMM)
0000-0002-4166-0449 (AOOr)
0000-0002-2340-3174 (PK)
0000-0001-8765-7766 (AOOy)

INTRODUCTION

Diabetes mellitus, often known as diabetes or DM, is a collection of metabolic diseases that exacerbate the onset of persistent hyperglycemia and are closely linked to the degeneration of the pancreatic β cells that produce insulin (Todd, 2010). In the previous few decades, type 1 diabetes has been viewed as a disorder in children and adolescents, but this has changed. These days, this condition has no age restrictions and is regarded as the most important disorder globally. An autoimmune condition linked to a compromised adaptive immune system is type 1 diabetes. There is a direct correlation between having type 1 diabetes and the eventual likelihood of developing type 2 diabetes (Blind et al., 2018). A little over 537 million persons had diabetes in 2021, and 6.7 million deaths were reported in this time frame. Up to 783 million people worldwide are predicted to have diabetes by the end of 2045, and an additional 481 million will have impaired glucose tolerance (IDF, 2016). Ninety percent of all cases of DM are categorized as type 2. The genetic background of patients and medical history might influence a variety of pathophysiological and clinical circumstances that complicate the diagnosis and treatment of type 2 diabetes. There have been a number of negative consequences reported, such as weight gain and hypoglycemia, but one characteristic that has not been addressed is the inability to enhance long-term beta cell activity. It is, therefore, critically necessary to lift the burden of diabetes and its excitement components. Plants have been reported to have secondary metabolites with strong anti-hyperglycemic actions and minimal adverse effects (Gothai et al., 2016).

The plant *Cyperus sexangularis* Nees (family *Cyperaceae*) is a tufted, long-lasting (perennial) sedge and is mostly native to the wetland environment (Raimondo et al., 2009). It has been reported that the other species of *Cyperus,* i.e., *Cyperus rotundus,* have anti-diabetic properties (Raut and Gaikwad, 2006; Singh et al., 2015). To the best of our knowledge, the hypoglycemic properties of the phytocompounds in *C. sexangularis* leaf extracts are yet to be determined. Our previous study reported the antioxidant, anti-inflammatory, and anti-elastase compounds from *C. sexangularis* (Miya et al., 2023). Therefore, in this study, we used the molecular docking approach to determine the specific binding modes of action of the reported compounds against α-amylase and α-glucosidase proteins, drug-likeness profiling, and molecular dynamics-based approaches to investigate the antidiabetic properties of the isolated phytocompounds, namely β-sitosterol, stigmasterol (steroids), dodecanoic acid (fatty acid), ethyl nonadecanoate, and ethyl stearate (fatty acid esters) from *C. sexangularis* leaf for the first time.

MATERIAL AND METHODS

Chemicals and general experimental procedure

Reagents and solvents were of analytical grade, purchased from Sigma-Aldrich (Pty) Ltd., Johannesburg, South Africa. Silica gel for TLC and column chromatography was procured from Merck (Pty) Ltd., Johannesburg, South Africa. Silica gel 60 F_{254} (Merck KGaA, Darmstadt, Germany) for thin-layer chromatography (TLC), and Silica gel 60, 0.060-0.2 mm (70-230 mesh) (Merck Millipore, Burlington, MA, United States) for column chromatography (CC) were used. Absorbance was read on the 680-Bio-Rad microplate reader with serial number 14966 (Bio-Rad Laboratories, Inc., Hercules, CA, USA). Spectroscopic analysis of the isolated compounds was performed on a 400 MHz Varian NMR spectrometer (Varian, Inc., Palo Alto, CA, USA) and 600 MHz Bruker Biospin GmbH spectrometer (Bruker BioSpin GmbH & Co. KG, Etlingen, Germany), with tetramethyl silane (TMS) as the NMR internal standard. Chemical shift (δ) was recorded in parts per million (ppm), with isolated compounds run in deuterated benzene (Sigma-Aldrich, St Louis, MO, USA). The molecular mass of each compound was determined by the electron-spray-ionization method (HRESI-MS) on a Quadrupole Time-of-Flight (QToF) Synapt G2 mass spectrometer (Waters Corporation, Milford, MA, USA). The mass-to-charge ratio of each fragment was recorded in m/z at a scan range of m/z 100-1000.

Plant material and extraction method

The leaf sheaths of *C. sexangularis* were collected from the Botanical Garden in the Limpopo Province (latitude: 22.6823° S, longitude: 29.1012° E). An herbarium specimen was deposited in the Department of Botany Herbarium at the University of Pretoria, South Africa, with a voucher number MGM 008. The leaf sheaths were air-dried at room temperature (≈25°C) and ground into powder. An amount of 0.7 kg of the leaf powder was extracted thrice in 7500 mL each of n-hexane (Hex), dichloromethane (DCM), ethyl acetate (EtOAc), and ethanol (EtOH) to afford Hex (83 g), DCM (19 g), EtOAc (8 g) and EtOH (68 g) extracts.

Chromatographic isolation and spectroscopic characterization of compounds

Based on the chromatographic separation method described by Miya et al. (2023), three and two compounds were isolated from C. sexangularis DCM and n-hexane extracts, respectively. Here, the DCM ex-

tract was adsorbed to 60 g of silica gel. The adsorbed extract was dry packed on a 200 g silica gel glass column of 600 × 50 mm (length × internal diameter) dimension. Thereafter, the column was eluted with solvent systems of increasing level of polarity as thus: Hex (100%), Hex-DCM (90:10, 80:20, 70:30, 60:40, 50:50, 40:60, 30:70, 20:80 and, 10:90%), DCM (100%), DCM-EtOAc (90:10, 80:20, 70:30, 60:40,50:50, 40:60, 30:70, 20:80 and, 10:90%), EtOAc (100%), EtOAc-MeOH (95:5, 90:10, 80:20, and 50:50%) and MeOH (100%). The elution process afforded three compounds. The procedure was repeated for the n-hexane extract to afford two compounds. The purity and class of isolated compounds were ascertained using the TLC phytochemical screening method (Harborne, 1998), while the structures of the isolated compounds were elucidated by spectroscopic means. The LC-MS/MS chromatograms of the extracts and the isolated compounds are indicated as supplementary data (Figs. S1–S7).

In silico molecular docking

Preparation and refinement of the protein and ligand structures

The phytocompounds were docked against proteins known to play important roles in diabetes. The protein of choice in this case is called α-amylase and α-glucosidase, and it is a crucial therapeutic target for diabetics. From the Protein Data Bank (http://www.rcsb.org), the PDB structure of α-amylase (PDB ID 5E0F; 1.40 Å resolution) (Caner and Brayer, 2016) and α-glucosidase (PDB ID 5NN6; 2.00 Å resolution) (Roig-Zamboni et al., 2017) was obtained. Before analysis, the corresponding protein structures of the related inhibitor (native ligand) and water molecules were cleared. Polar hydrogen atoms and Kollman charges were added to the protein structures to prepare them for docking in AutoDockTools.

The concerned phytocompounds were downloaded from the NCBI PubChem (https://pubchem.ncbi.nlm.nih.gov/). The Open Babel Server was then used to transform the downloaded sdf structures into pdb structures (O'Boyle et al., 2011). The ligand structures underwent energy minimization using the Gromos 96 force field after the PRODRG server (Schüttelkopf and Van Aalten, 2004) was used to optimize their energy.

Determination of the active site and molecular docking

The literature (Caner and Brayer, 2016; Roig-Zamboni et al., 2017) was used to predict the active site of the proteins (α-amylase and α-glucosidase). The CASTp 3.0 (Computed Atlas of Surface Topography of Proteins) online server (Binkowski et al., 2003) was used to validate the predictions. The top result from the top three possible ligand-binding sites was selected for docking after the processed protein without a native inhibitor was submitted to the CASTp 3.0 server. Then, the amino acids at the active sites of the native inhibitor-α-amylase co-crystallized complex and native inhibitor-α-glucosidase co-crystallized complex were compared with the amino acid residues predicted by CASTp 3.0. In order to confirm the active site, this was accomplished by manually opening the co-crystallized complex in the Discovery studio visualization tool (Kar et al., 2022a; 2022b). As a result, the interacting residues could be identified and were discovered to be fairly close to those that the CASTp 3.0 server had predicted. For each atom of the native inhibitor ligand, grid maps (X, Y, and Z confirmations; Box center and Box dimension) were created using the Autodock and Autogrid tools connected with Autodock4. Molecular docking was performed using the Autodock4 to obtain the X, Y, and Z confirmations (Box center and Box dimension) as a possible target location. A stiff protein receptor and a flexible ligand docking methodology were used to molecularly dock the ligands of interest at the active binding sites of the relevant proteins using a grid-based molecular docking technology (Kar et al., 2021; 2022a; 2022b). A grid box involving the active site residues of the α-amylase protein was created, with center_x = -7.2, center_y = 5.7, center_z = -23.1, size_x = 22.6, size_y = 21.1, and size_z = 22.7. Similarly, a grid box covering the active binding pocket of α-glucosidase was employed, with center_x = -14.3, center_y = -32.0, center_z = 95.8, size_x = 16.9, size_y = 15.3, and size_z = 14.7. After Autodock Vina finished the molecular docking procedure, the docked complexes were visualized using the Discovery Studio visualization tool (Kar et al., 2022a; 2022b). Protein-Ligand Interaction Profiler (PLIP) web server (Salentin et al., 2015) and PyMol (version 1.7.4) software were used to perform interaction profiling and analysis on ligand-receptor complexes with the lowest binding scores and RMSD < 2.0 A (Naidoo et al., 2020).

Validation of docking protocol by redocking

The conformation of the native ligand, which was bound to the active site of the protein, was identified. In addition, the conformation of the new ligand (stigmasterol and β-sitosterol) bound at the active site of the protein was also identified. The conformation of the native and new ligands was matched through superimposition (Joshi et al., 2014; Saleh-E-In et al., 2019).

Assessment of physicochemical features and potential toxicity of the phytocompounds

For additional physicochemical properties and drug-like feature evaluation, the phytocompounds with the corresponding proteins in AutoDock Vina were selected (Naidoo et al., 2020). The SwissADME server was utilized to estimate the physicochemical parameters, and the pkCSM server was used for validation (Daina et al., 2017; Pires et al., 2015). The compounds' pharmacokinetic features (human intestinal absorption and oral bioavailability) and potential toxicity (cytotoxicity, carcinogenicity, hepatotoxicity, mutagenicity (AMES mutagenesis), and P-glycoprotein inhibitor) were evaluated using the ProTox-II and vNN-ADMET online servers (Banerjee et al., 2018; Schyman et al., 2017).

Molecular dynamics simulations

Molecular dynamics simulation (MDS) helps to precisely evaluate the possible stability of protein-ligand complexes and is a crucial step in confirming molecular docking results (Kar et al., 2021). The compounds were subjected to MDS for 120 ns using the GROMACS (version 2019) force field parameters (GROMOS96 43a1) (Abraham et al., 2015; Kar et al., 2021; 2022a; 2022b). Constant pressure and temperature (NPT) ensemble was used to set the equilibration stages (Elfiky and Azzam 2020; Enayatkhani et al., 2020; Umesh et al., 2020). According to Umesh et al. (2020), the MD simulations were run at a standard temperature of 300 K and pressure of 1.013 bar. An estimate of the conformational and structural stability of complexes was obtained through the analysis of root-mean-square-deviation/fluctuation (RMSD/F).

RESULTS AND DISCUSSION

Structure elucidation of the phytocompounds

The elucidation of compounds was based on spectroscopic evidence, as previously discussed by Miya et al. (2023). Thus, the compounds were identified as dodecanoic acid, ethyl nonadecanoate, and ethyl stearate from the DCM extract, while β-sitosterol and stigmasterol were isolated from the *n*-hexane extract of the plant.

Dodecanoic acid ($C_{12}H_{24}O_2$)

^{1}H NMR (400 MHz in C_6D_6), δ ppm: 0.86 (3H, *t, J* = 8.0, 8.0 Hz, H-12), 1.23–1.28 (2H, *m*, H-3 to H-10), 1.58 (2H, *t, J* = 9.6, 7.6 Hz, H-2); ^{13}C NMR (150 MHz in C_6D_6), δ ppm: 179.8 (C-1), 31.9 (C-2), 29.4 (C-3), 29.9 (C-4/C-5/C-6/C-7/C-8, C-9), 29.9 (C-10), 22.9 (C-11), 14.1 (C-12).

Ethyl nonadecanoate ($C_{21}H_{42}O_2$)

^{1}H NMR (600 MHz in C_6D_6), δ ppm: 0.91 (3H, *t, J* = 6.9 Hz, H-19), 1.26 (3H, *t, J* = 16.4 Hz, H-20), 2.21 (2H, *t, J* = 7.4 Hz, H-2), 4.07 (2H, *t, J* = 6.7 Hz, H-10); ^{13}C NMR (150 MHz in C_6D_6), δ ppm: 173.0 (C-1), 34.6 (C-2), 25.5 (C-3), 26.4 (C-4), 29.3 (C-5), 29.6 (C-6), 29.7 (C-7), 29.7 (C-8), 29.9 (C-9), 29.8 (C-10), 30.1 (C-11), 30.0 (C-12), 30.1 (C-13), 30.1 (C-14), 30.2 (C-15), 30.2 (C-16), 32.4 (C-17), 23.1 (C-18), 14.0 (C-19), 64.3 (C-10), 14.3 (C-20).

Ethyl stearate ($C_{20}H_{40}O_2$)

^{1}H NMR (600 MHz in C_6D_6), δ ppm: 0.91 (3H, *t, J* = 6.8 Hz, H-18), 1.26 (3H, *t, J* = 21.6 Hz, H-20), 2.21 (2H, *t, J* = 7.4 Hz, H-2), 4.08 (2H, *dd, J* = 6.7, 6.7 Hz, H-10); ^{13}C NMR (150 MHz in C_6D_6), δ ppm: 173.0 (C-1), 34.6 (C-2), 25.5 (C-3), 26.4 (C-4), 29.3 (C-5), 29.6 (C-6), 29.7 (C-7), 29.7 (C-8), 29.9 (C-9), 29.8 (C-10), 30.1 (C-11), 30.0 (C-12), 30.1 (C-13), 30.1 (C-14), 30.2 (C-15), 32.4 (C-16), 23.1 (C-17), 14.3 (C-18), 64.3 (C-10), 14.3 (C-20).

β-sitosterol ($C_{29}H_{50}O$)

^{1}H NMR (400 MHz in C_6D_6), δ ppm: 0.66 (3H, *s*, H-19), 0.78 (3H, *d, J* = 4.0 Hz, H-29), 0.80 (3H, *d, J* = 4.0 Hz, H-28), 0.82 (3H, *t, J* = 4.5, H-26), 0.91 (3H, *d, J* = 6.4 Hz, H-21), 0.99 (3H, *s*, H-18), 2.25 (2H, *d, J* = 6.8 Hz, H-4), 3.52 (1H, *tdd, J* = 9.6, 6.4, 6.0 Hz, H-3), 5.32 (1H, *bd, J* = 5.2 Hz, H-6); ^{13}C NMR (100 MHz in $CDCl_3$), δ ppm: 37.5 (C-1), 31.9 (C-2), 71.8 (C-3), 42.3 (C-4), 140.7 (C-5), 121.4 (C-6), 30.4 (C-7), 29.7 (C-8), 50.0 (C-9), 36.9 (C-10), 22.9 (C-11), 39.5 (C-12), 42.3 (C-13), 56.6 (C-14), 28.1 (C-15), 29.7 (C-16), 55.8 (C-17), 11.8 (C-18), 17.9 (C-19), 36.2 (C-20), 19.2 (C-21), 35.6 (C-22), 25.7 (C-23), 45.7 (C-24), 24.3 (C-25), 11.9 (C-26), 29.7 (C-27), 20.9 (C-28), 19.3 (C-29).

Stigmasterol ($C_{29}H_{48}O$)

^{1}H NMR (600 MHz in $CDCl_3$), δ ppm: 0.68 (3H, *s*, H-19), 0.80 (3H, *d, J* = 6.9 Hz, H-29), 0.82 (3H, *d, J* = 6.9 Hz, H-28), 0.84 (3H, *t, J* = 8.1 Hz, H-26), 0.92 (3H, *d, J* = 6.7 Hz, H-21), 1.00 (3H, *s*, H-18), 3.53 (1H, *dt, J* = 6.0 Hz, H-3), 5.35 (1H, *bd, J* = 6.0 Hz, H-6); ^{13}C NMR (150 MHz in $CDCl_3$), δ ppm: 37.4 (C-1), 34.1 (C-2), 71.9 (C-3), 42.42 (C-4), 140.9 (C-5), 121.9 (C-6), 31.8 (C-7), 32.0 (C-8), 50.3 (C-9), 36.3 (C-10), 21.2 (C-11), 39.9 (C-12), 42.5 (C-13), 56.9 (C-14), 24.5 (C-15), 29.3 (C-16), 56.2 (C-17), 12.1 (C-18), 18.9 (C-19), 40.6 (C-20), 19.9 (C-21), 138.5 (C-22), 129.4 (C-23), 45.9 (C-24), 26.2 (C-25), 12.0 (C-26), 29.9 (C-27), 19.5 (C-28), 19.2 (C-29).

The LC-MS/MS chromatograms of isolated compounds are presented as supplementary data (Figs. S1–S7).

Table 1. Binding energy scores and interaction profile of the phytocompounds with α-amylase.

Phytocompounds	Binding energy scores (kcal/mol)	Interacting residues
	α-amylase protein (5E0F)	
Dodecanoic acid	-5.8 ± 0.02	*Trp58, Trp59, Tyr62, Leu165,* His 101#
Ethyl nonadecanoate	-6.1 ± 0.04	*Trp58, Trp59, Tyr62*
Ethyl stearate	-6.3 ± 0.03	*Trp58, Trp59, Tyr62, Gln63, Leu162, Leu165, Ala198,* His 201#
β-Sitosterol	-10.0 ± 0.01	*Trp59, Tyr62, Gln63, Leu162, Thr163, Leu165, Ala198*
Stigmasterol	-10.0 ± 0.02	*Trp58, Trp59, Tyr62, Gln63, Leu165*
5,7-dihydroxy-4-oxo-2-(3,4,5-trihydroxyphenyl)-4H-chromen-3-yl 6-deoxy-2-O-{6-O-[(2E)-3-(3,4-dihydroxyphenyl)prop-2-enoyl]-beta-D-glucopyranosyl}-alpha-L-mannopyranoside (native ligand)	-11.5 ± 0.01	*Leu162, Leu165,* **Trp59, Gln63, Lys200, His201*, Glu233, His305*, Asp356**
Acarbose	-8.6 ± 0.01	*Trp58, Ile235,* **Gln63, Ala198, His201, Glu233, His305**

Hydrophobic interactions are marked in italics, hydrogen bonds are highlighted in bold, π-stakings are displayed with *, and salt bridges are displayed with #.

Table 2. Binding energy scores and interaction profile of the phytocompounds with α-glucosidase.

Phytocompounds	Binding energy scores (kcal/mol)	Interacting residues
	α-glucosidase protein (5NN6)	
Dodecanoic acid	-6.1 ± 0.02	*Trp376, Leu405, Trp481, Trp516, Trp613, Phe649*
Ethyl nonadecanoate	-5.8 ± 0.04	*Trp376, Trp481, Trp516, Phe525, Trp613, Phe649, Leu650, Leu677, Leu678*
Ethyl stearate	-5.5 ± 0.03	*Trp376, Trp481, Trp516, Phe525, Trp613, Phe649, Leu650, Leu677, Leu678*
β-Sitosterol	-6.6 ± 0.01	*Trp376, Trp481, Phe525, Phe649,* **His674**
Stigmasterol	-7.6 ± 0.02	*Trp376, Trp481, Phe525, Phe649,* **Asp518**
(2R,3R,4R,5S)-1-(2-hydroxyethyl)-2-(hydroxymethyl)piperidine-3,4,5-triol (native ligand)	-4.4 ± 0.02	**Trp481, Asp616#, His674,** Asp404#, Asp518#
Acarbose	-4.6 ± 0.02	***Trp481****, Phe525,* **Arg600, Trp613, Asp616**

Hydrophobic interactions are marked in italics, hydrogen bonds are highlighted in bold, π-stakings are displayed with *, and salt bridges are displayed with #.

In silico molecular docking

Phytochemicals extracted from the leaf extract of *C. sexangularis* were subjected to molecular docking against the diabetes-associated proteins α-amylase and α-glucosidase. The digestive enzyme α-amylase raises blood and postprandial glucose levels by dissolving polysaccharide molecules into glucose and maltose (Kaur et al., 2021). On the other hand, the small intestine's α-glucosidase breaks down carbohydrates into glucose in the digestive tract. They are essential for chemical synthesis, alcohol fermentation, and the body's metabolism (Assefa et al., 2019). Conversely, in diabetic patients, there is a discernible correlation between α-amylase and α-glucosidase and the adsorption of glucose. Thus, limiting the action of the enzymes that break down carbohydrates, namely α-amylase and α-glucosidase, is a new approach to reduce the absorption of carbohydrates from food, reduce postprandial hyperglycemia, and postpone the onset of diabetes. Two phytosterols that are frequently present in plant cell membranes are stigmasterol and β-sitosterol. A wide class of organic substances known as "plant steroids" is necessary for the development, reproduction, and adaptation of plants to different kinds of stress (Yerlikaya et al., 2023). Numerous phytosterols have demonstrated intriguing pharmacological properties as strong inhibitors of enzymes. According to Poulose et al. (2021), the seaweed *Gelidium spinosum* contains stigmasterol, which may have the ability to suppress the activity of α-amylase. On the other hand, Manigandan and Subramaniyan (2021) reported that the phytosterol β-sitosterol that was isolated from *Andrographis echioides* inhibited the enzymes α-amylase and α-glucosidase. Tables 1 and 2 provide comprehensive

details about the binding energy scores of the compounds with the α-amylase and α-glucosidase proteins. The interaction of steroid phytocompound stigmasterol with the hydrophobic interactions (Trp58, Trp59, Tyr62, Gln63, Leu165) of the α-amylase protein displayed the binding energy score of -10.0 kcal/mol. It was evident that hydrophobic interactions (Trp59, Tyr62, Gln63, Leu162, Thr163, Leu165, Ala198) of the protein α-amylase with another steroid compound β-sitosterol returned a binding energy score of -10.0 kcal/mol (Fig. 1A-B). The standard acarbose showed a binding energy score of -8.6 kcal/mol with hydrogen bond interactions (Gln63, Ala198, His201, Glu233, His305) and hydrophobic interactions (Trp58, Ile235). In this investigation, we examined how the suggested inhibitor (native ligand) 5,7-dihydroxy-4-oxo-2-(3,4,5-trihydroxyphenyl)-4H-chromen-3-yl 6-deoxy-2-O-{6-O-[(2E)-3-(3,4-dihydroxyphenyl)prop-2-enoyl]-beta-D-glucopyranosyl}-alpha-L-mannopyranoside (Caner and Brayer, 2016) bound to the α-amylase protein and contrasted it with the phytochemicals' binding patterns that were of interest. With a binding energy value of -11.5 kcal/mol, the inhibitor (native ligand) demonstrated a substantial binding potential and implicated the residues Leu162, Leu165 (hydrophobic interactions), Trp59, Gln63, Lys200, His201, Glu233, His305, and Asp356 (hydrogen bonds) at the α-amylase's active binding pocket (Table 1). It is interesting to note that these active site residues are implicated in the substances stigmasterol, β-sitosterol and acarbose (Table 1 and Fig. 1A-C), which have been proposed to be important in the interaction between α-amylase and small molecule inhibitors (Caner and Brayer, 2016).

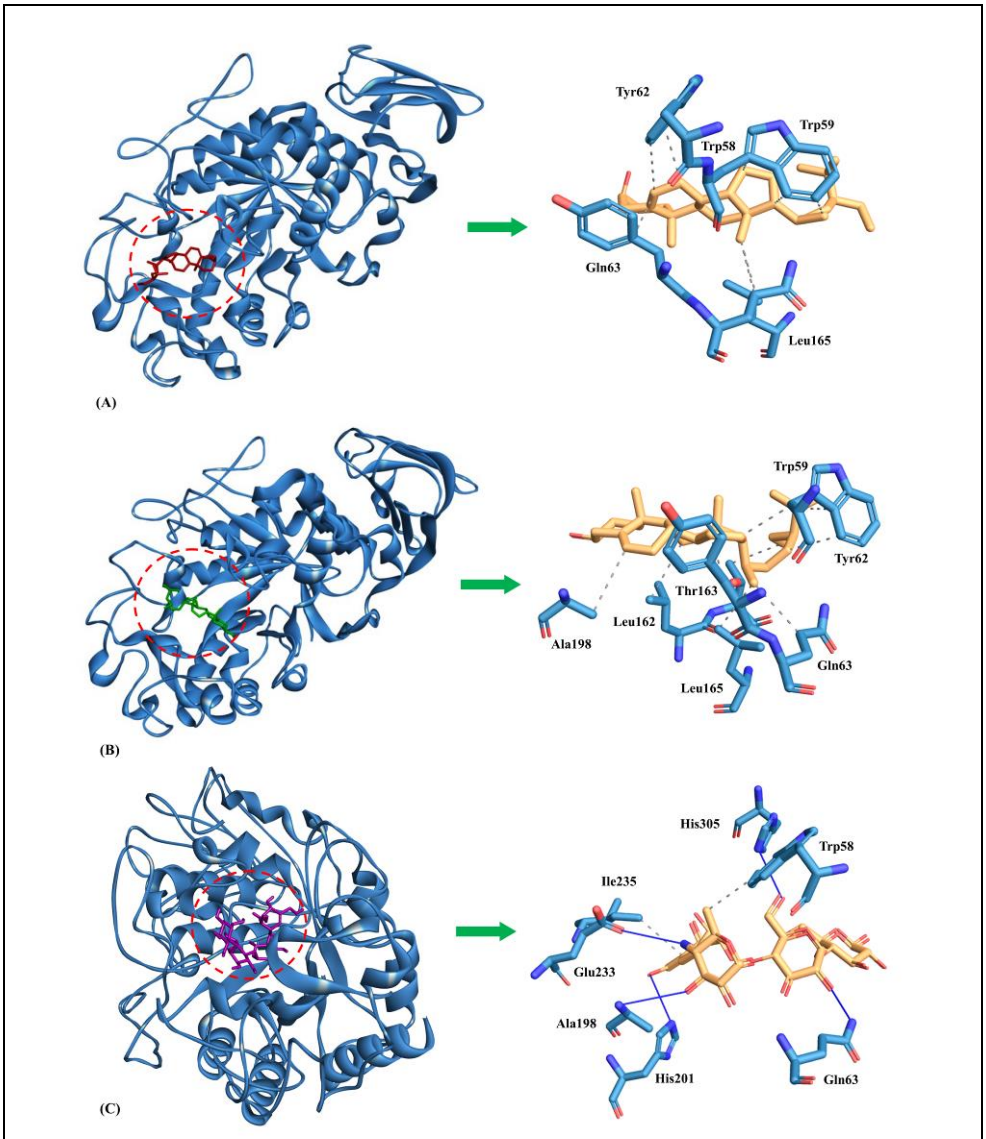


Figure 1. The mode of interaction of **(A)** stigmasterol, **(B)** β-sitosterol, and **(C)** acarbose with α-amylase protein.

The blue ribbon represents the α-amylase protein. Stigmasterol, β-sitosterol, and acarbose have been illustrated as red, green, and pink sticks. Gray dashed lines represent hydrophobic interactions, respectively.

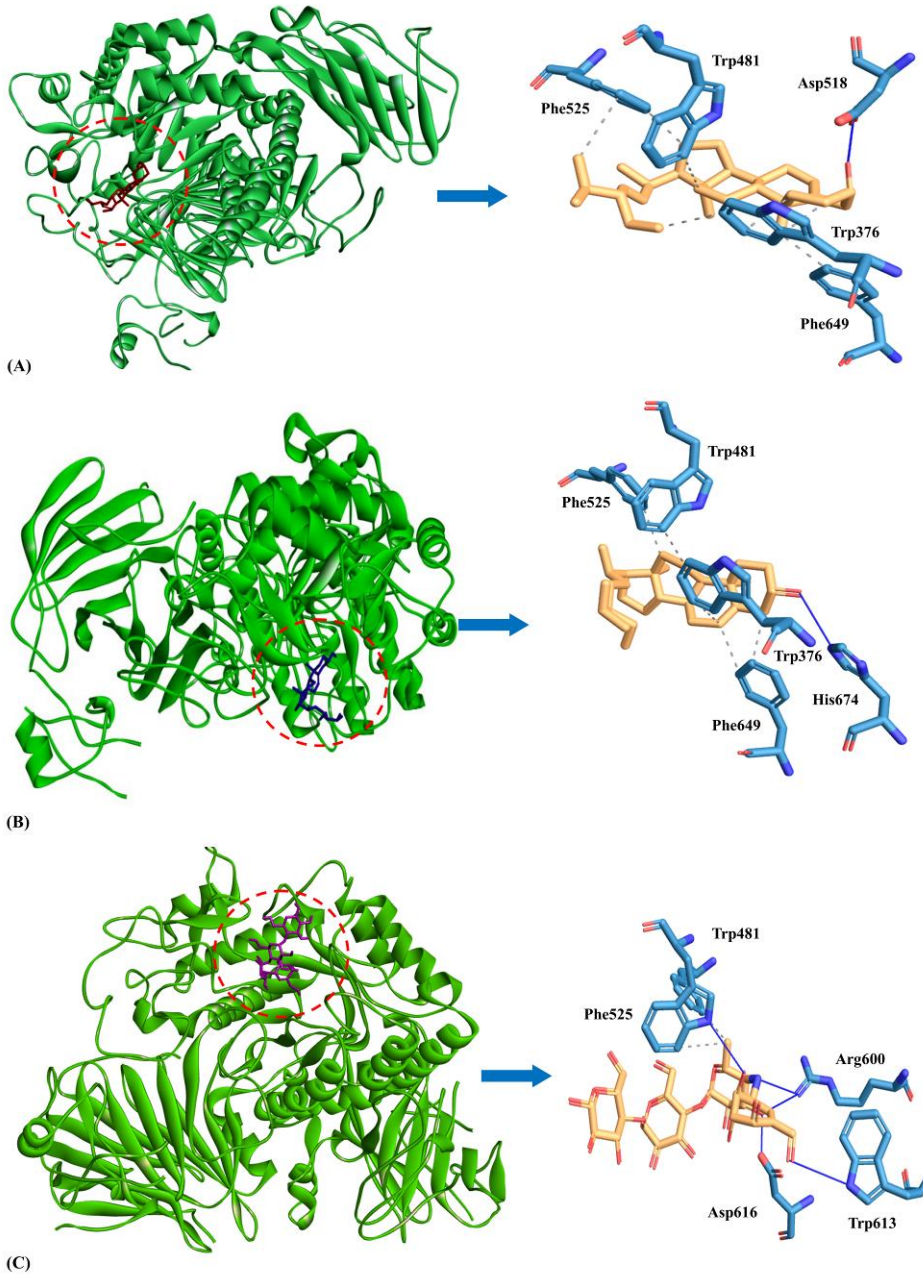


Figure 2. The mode of interaction of **(A)** stigmasterol, **(B)** β-sitosterol, and **(C)** acarbose with α-glucosidase protein.

The green ribbon represents the α-glucosidase protein. Stigmasterol, β-sitosterol, and acarbose have been illustrated as a red, blue, and pink stick. Gray dashed and blue solid lines represent hydrophobic and hydrogen bonds, respectively.

The compound stigmasterol interacts with the hydrophobic interaction (Trp376, Trp481, Phe525, Phe649) and hydrogen bond interactions (Asp518) of the protein α-glucosidase returning a binding energy score of -7.6 kcal/mol. On the other hand, β-sitosterol interaction with α-glucosidase (hydrophobic interaction: Trp376, Trp481, Phe525, Phe649 and hydrogen bonds: His674) displayed an energy score of -6.6 kcal/mol (Table 2 and Fig. 2A-B). Hydrophobic and hydrogen bond interactions resulted in a binding energy score of -4.6 kcal/mol for the standard acarbose (Fig. 2C). Interestingly, the binding potential of stigmasterol and β-sitosterol was significantly higher than that of the suggested inhibitor (2R,3R,4R,5S)-1-(2-hydroxyethyl)-2-(hydroxymethyl) piperidine-3,4,5-triol (Table 2) (Roig-Zamboni et al., 2017). The active site residues Trp481, His674, and Asp518 of α-glucosidase were clearly involved in the interactions between stigmasterol and β-sitosterol and the enzyme, which is essential for binding the putative

inhibitor. Therefore, it stands to reason that stigmasterol and β-sitosterol may have a considerable capacity to bind and inhibit α-glucosidase (Roig-Zamboni et al., 2017).

Redocking and superimposition

Redocking was performed to validate the docking protocol. It was interesting to note that the α-amylase protein's native conformation and the re-docked conformation of 5,7-dihydroxy-4-oxo-2- (3,4,5-trihydroxyphenyl)-4H-chromen-3-yl6-deoxy-2-O-{6-O-[(2E)-3-(3, 4-dihydroxyphenyl) prop-2-enoyl]-beta-D-glucopyranosyl}-alpha-L-mannopyranoside (native ligand) with α-amylase protein produced the same hydrogen bonds (Glu233), hydrophobic interactions (Ala198, Thr163, Trp58, Lys200), and Pi-Pi stacked (Leu162, Leu165, Ile235) (Fig. 3A-B). On the other hand, α-glucosidase native conformation and the native ligand re-docked with α-glucosidase protein produced the same hydrogen bonds (Trp481, His674, Asp616), and hydrophobic interactions (Phe525, Met519, Leu405, Trp613, Trp516, Phe649, Trp376) (Fig. 4A-B). The docking program could be employed because of the reproducibility of significant interactions. This demonstrated the docking protocol's effectiveness and legitimacy (Joshi et al., 2014).

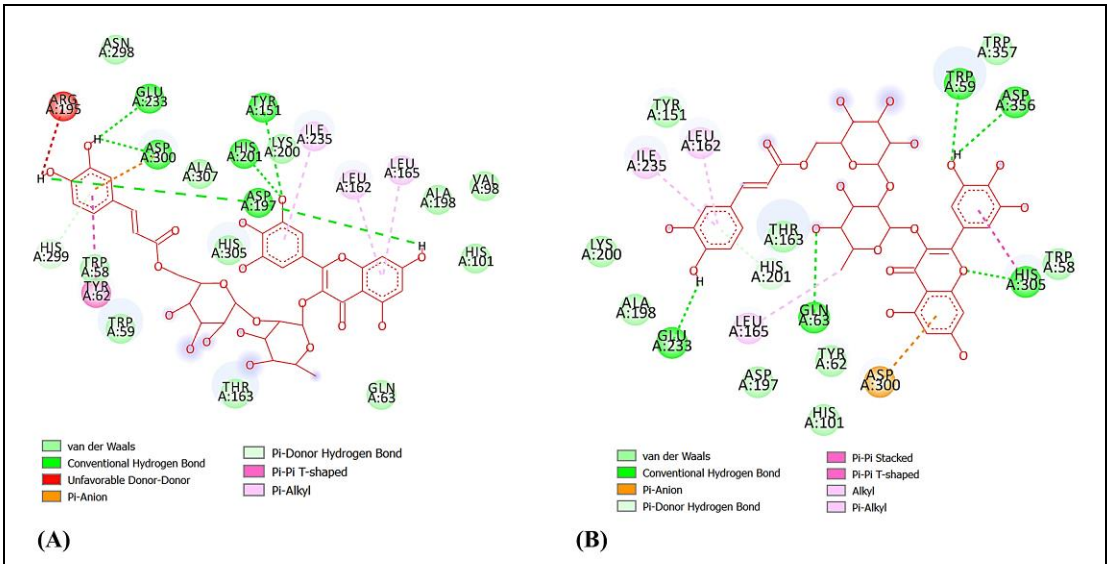


Figure 3. Validation of docking protocol **(A)** α-amylase protein's co-crystal structure native conformation, and **(B)** re-docked with co-crystal structure's native inhibitor ligand with α-amylase protein.

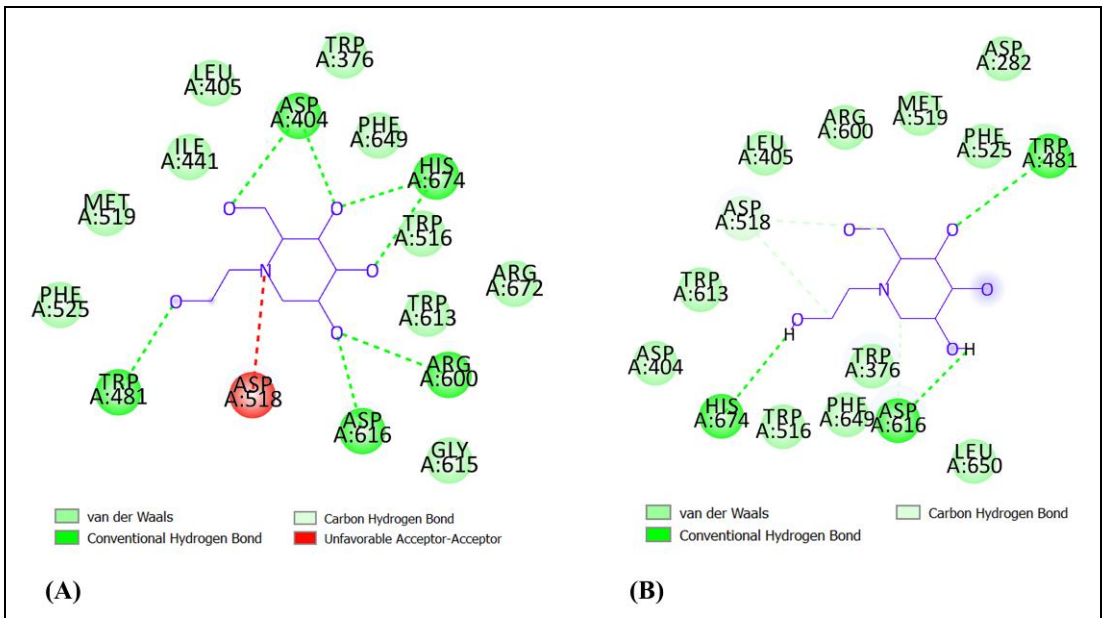


Figure 4. Validation of docking protocol **(A)** α-glucosidase protein's co-crystal structure native conformation, and **(B)** re-docked with co-crystal structure's native inhibitor ligand with α-glucosidase protein.

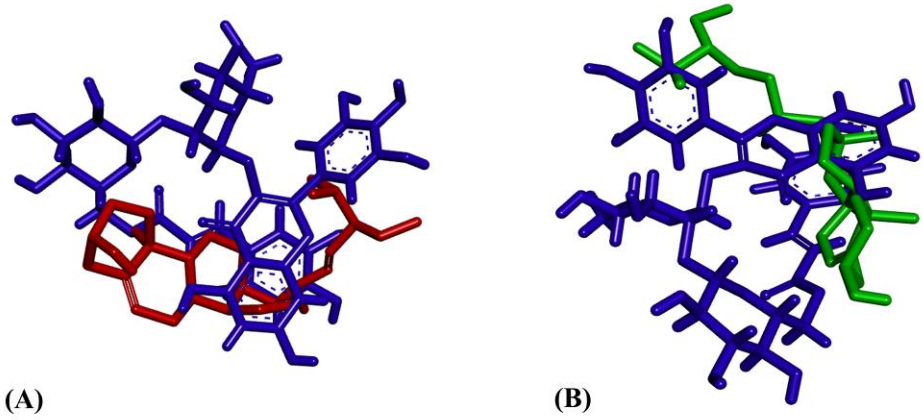


Figure 5. (A) Redocked ligand stigmasterol (red) superimpose to native ligand (blue) of α-amylase, and **(B)** re-docked ligand β-sitosterol (green) superimpose to native ligand (blue) of α-amylase.

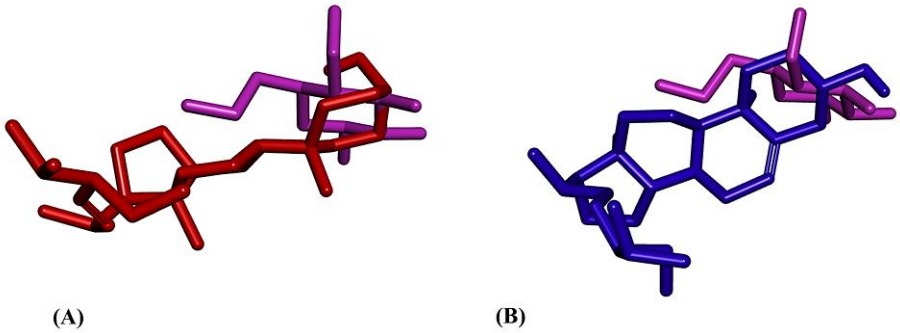


Figure 6. (A) Redocked ligand stigmasterol (red) superimpose to native ligand (pink) of α-glucosidase, and **(B)** re-docked ligand β-sitosterol (blue) superimpose to native ligand (pink) of α-glucosidase.

It was found that the docked complex (stigmasterol-α-amylase, β-sitosterol-α-amylase, and stigmasterol-α-glucosidase, β-sitosterol-α-glucosidase) was superimposed completely onto the native co-crystallized α-amylase and α-glucosidase protein complex without any adjustments. The atoms of amino acids of both the complexes (stigmasterol-α-amylase, β-sitosterol-α-amylase) were superimposed with the native co-crystallized α-amylase protein without any constraints. Conversely, the amino acid atoms of both the complexes (stigmasterol-α-glucosidase, β-sitosterol-α-glucosidase) were likewise overlaid with the native co-crystallized α-glucosidase protein. Figs. 5A-B and 6A-B display the superimposed images of the co-crystal structure's native ligand and the re-docked ligands (stigmasterol, β-sitosterol) (Gentile et al., 2020; Yanuar et al., 2018). The findings suggest that the phytocompounds stigmasterol and β-sitosterol, also precisely bind to the amino acids found in the active site cleft of the α-amylase and α-glucosidase proteins.

Physicochemical properties of the phytochemicals and accordance with the rules of drug-likeness

A possible treatment candidate's physicochemical characteristics are thought to be closely related to its therapeutic efficacy, safety, and efficient metabolism (Doak et al., 2014; Gleeson et al., 2011). For the phytochemicals extracted from the *n*-hexane and DCM leaf extracts of *C. sexangularis*, several characteristics such as molecular weight (MW [Dalton]), number of hydrogen bond acceptors (HBA), and donors (HBD), number of rotable bonds, topological polar surface area (TPSA), and logarithm of partial coefficient (log P) were meticulously estimated. The physical-chemical characteristics were assessed using the standard drug-likeness guidelines used in the early phases of drug discovery, specifically Lipinski's rule of five (RO5) and Veber's rule. Lipinski's rule of five proposes that a drug candidate with a logarithm of partial coefficient (log P) ≤ 5, molecular weight ≤ 500 Dalton, number of hydrogen bond acceptors ≤ 10, and number of hydrogen bond donors ≤ 5 exhibits decent gastrointestinal absorption and enhanced membrane permeability (Lipinski et al., 2001). According to Veber et al. (2002), a medicinal molecule should have good oral bioavailability if its TPSA is less than 140 Å

and its number of rotatable bonds is less than 10. The physicochemical features of the compounds were compared with the relevant standard drug acarbose with a motive to infer the potential druggability of the compounds in relevance to the drugs. Physicochemical properties of the concerned phytochemicals like dodecanoic acid, β-sitosterol, and stigmasterol were found to be in perfect accordance with Lipinski's rule of Five (RO5) and Veber's rule, signifying their considerable drug-like potential (Table 3).

Analysis of pharmacokinetic features and potential toxicity

The term "drug absorption" describes how a medication gets from its extravascular delivery site to the bloodstream, where it can travel to its intended site of action (Lagorce et al., 2017). According to an *in silico* evaluation of intestinal absorption, the human gastrointestinal tract can absorb all of the phytochemicals to a high degree (Table 4). According to earlier research (Petit et al., 2016; Wang et al., 2017), our findings of significant intestine absorption for stigmasterol and β-sitosterol appeared to be justified. Based on the prediction techniques developed by Egan et al. (2000) and Veber et al. (2002), decent oral bioavailability was clearly demonstrated for all compounds (Table 4).

One of the most important things in the field of drug development is having the right knowledge and doing studies about the clinical safety of a novel therapeutic candidate (Blomme and Will, 2016). At a later stage of drug development, attrition related to drug toxicity is a significant barrier that results in the rejection of many therapeutic components (Waring et al., 2015). Major adverse consequences such as carcinogenicity, mutagenicity, hepatotoxicity, and tumorigenicity have been topics of great concern following the effective delivery of pharmaceuticals in the human system (Benigni and Bossa, 2011). Consequently, it has been proposed that in the early stages of drug development, *in silico* toxicity prediction and assessment of novel therapeutic candidates may be significant (Wang et al., 2017). According to Kroes et al. (2004), carcinogens are chemicals or mixtures that promote the development, expansion, and growth of tumors. Based on a thorough *in silico* toxicity assessment, dodecanoic acid, and stigmasterol were found to have the potential to be non-carcinogenic (Table 5).

One essential screening phase in the medication development process is the identification of compounds with structural alarms. The term "toxicophores" refers to PAINS compounds (panassay interference compounds), which are known to interfere with biological assays, interact and damage DNA/proteins, and ultimately cause hepatotoxicity, carcinogenicity, and CYP inhibition, among other potentially dangerous outcomes (Baell, 2010; Pouliot and Jeanmart, 2016). The concerned phytochemicals passed the PAINS-related toxicity screening stage because it was discovered that they lacked any PAINS structural alerts (Table 5).

The term "mutagenicity" describes the risks of genetic mutation resulting from exposure to substances that cause these kinds of mutative effects (Ames et al., 1973). Using the ProTox-II web server, an *in silico* mutagenicity assessment was accomplished in association with the Ames mutagenicity dataset. The outcomes were subsequently verified by the use of admetSAR 2.0 (Yang et al., 2019). Remarkably, Table 5 indicates that every molecule was anticipated to be free of mutagenicity, cytotoxicity, and hepatotoxicity.

Table 3. Physicochemical properties of the phytochemicals isolated from *C. sexangularis* leaf extracts and their accordance with the rules of drug-likeness.

Physicochemical properties	Compounds					
	Dodecanoic acid	Ethyl nonadecanoate	Ethyl stearate	β-Sitosterol	Stigmasterol	Acarbose (standard)
Molecular weight (Dalton)	200.32	326.56	312.53	414.71	412.69	645.60
Number of hydrogen bond acceptor (HBA)	2	2	2	1	1	19
Number of hydrogen bond donor (HBD)	1	0	0	1	1	14
No. of rotatable bonds	10	18	17	6	5	9
TPSA (Å^2)	37.30	26.30	26.30	20.23	20.23	321.17
log P	3.99	7.20	6.8	8.02	7.80	-8.56
In accordance with Lipinski's rule of Five (RO5)	Yes	Yes; 1 violation	Yes; 1 violation	Yes	Yes	No; 3 violations
In accordance with Veber's rule	Yes	No; 1 violation	No; 1 violation	Yes	Yes	No; 1 violation

Mol. Wt: Molecular weight; TPSA: Topological Polar Surface Area; log P: Logarithm of partial coefficient.

Table 4. Pharmacokinetic properties of the concerned phytochemicals isolated from *C. sexangularis* leaf extracts.

Pharmacokinetic properties	Compounds					
	Dodecanoic acid	Ethyl nonadecanoate	Ethyl stearate	β-Sitosterol	Stigmasterol	Acarbose (standard)
HIA	High (93.379%)	High (90.885%)	High (91.228%)	High (94.464%)	High (94.970%)	Poor (4.172%)
Oral bioavailability (Veber)	Good	Moderate	Moderate	Good	Good	Good
Oral bioavailability (Egan)	Good	Moderate	Moderate	Moderate	Moderate	Moderate

HIA: Human intestinal absorption. HIA values (%) have been mentioned in parentheses. HIA > 80%: high absorption, and HIA < 25%: poor absorption.

Table 5. *In silico* toxicity assessment of the concerned phytochemicals isolated from *C. sexangularis* leaf extracts.

Toxicity assessment	Compounds					
	Dodecanoic acid	Ethyl nonadecanoate	Ethyl stearate	β-Sitosterol	Stigmasterol	Acarbose (standard)
Mutagenicity (AMES mutagenesis)	No	No	No	No	No	No
Cytotoxicity	No	No	No	No	No	No
Carcinogenicity	No	Yes	Yes	Yes	No	No
Hepatotoxicity	No	No	No	No	No	Yes
Medicinal Chemistry (PAINS)	0 alert	0 alert	0 alert	0 alert	0 alert	0 alert
P-glycoprotein inhibitor	No	No	No	Yes	Yes	No

PAINS: Pan-assay interference compounds.

P-glycoprotein (P-gp) is a transmembrane protein that is a member of the ABC-transporters family of transporters, which is responsible for the active transport of a large number of chemically varied chemicals out of cells. It has a strong correlation with the ADMET (absorption, distribution, metabolism, excretion, and toxicity) characteristics of pharmaceuticals and therapeutic candidates. It also helps to reduce toxicity by removing substances from cells and preventing intracellular buildup. P-gp inhibitors are compounds that obstruct or bypass the P-gp drug efflux pump, also known as P-gp efflux. P-gp inhibitors have the ability to change a drug's pharmacokinetics, which can improve metabolism, absorption, and distribution (Le et al., 2022). β-sitosterol and stigmasterol were the two appropriate P-gp inhibitors among the five compounds in this investigation, as determined by *in silico* screening (Table 5). Thus, the relevant phytocompounds, stigmasterol, and β-sitosterol showed promising drug-like properties and offered more opportunities for *in vitro* and *in vivo* validation toward the development of potent diabetic treatments.

Molecular dynamics simulations

Based on binding energy ratings, the substances stigmasterol and β-sitosterol interacted with the α-amylase and α-glucosidase proteins (Tables 1 and 2). This led to the execution of 120 ns molecular dynamics (MD) simulations of the corresponding protein-ligand complexes. The complexes, including stigmasterol-α-amylase protein complexes (complex 1), β-sitosterol-α-amylase protein (complex 2), stigmasterol-α-glucosidase protein (complex 3), and β-sitosterol-α-glucosidase (complex 4) had mean RMSD values of 0.85, 0.65, 0.77 and 0.9 Å respectively. In complexes 1, 2, 3, and 4, the RMSD values of the C atoms fluctuated initially, but after 101, 98, 92, and 105 ns, they stabilized and stayed in equilibrium (Fig. 7A, C, E, G). Our findings demonstrated that the complexes were stable in their shape and suggested that stigmasterol and β-sitosterol had a respectable capacity for binding when they interacted with the α-amylase and α-glucosidase proteins (Khan et al., 2020). To address local alterations along a protein chain and interpret the conformational stability of the complex, it is useful to analyze the root mean square fluctuation (RMSF) of the residues of a protein-ligand complex (Muralidharan et al., 2020). After a thorough examination of the RMSF values associated with the complexes, it was determined that the average values for the complexes stigmasterol-α-amylase protein complexes (complex 1), β-sitosterol-α-amylase protein (complex 2), stigmasterol-α-glucosidase protein

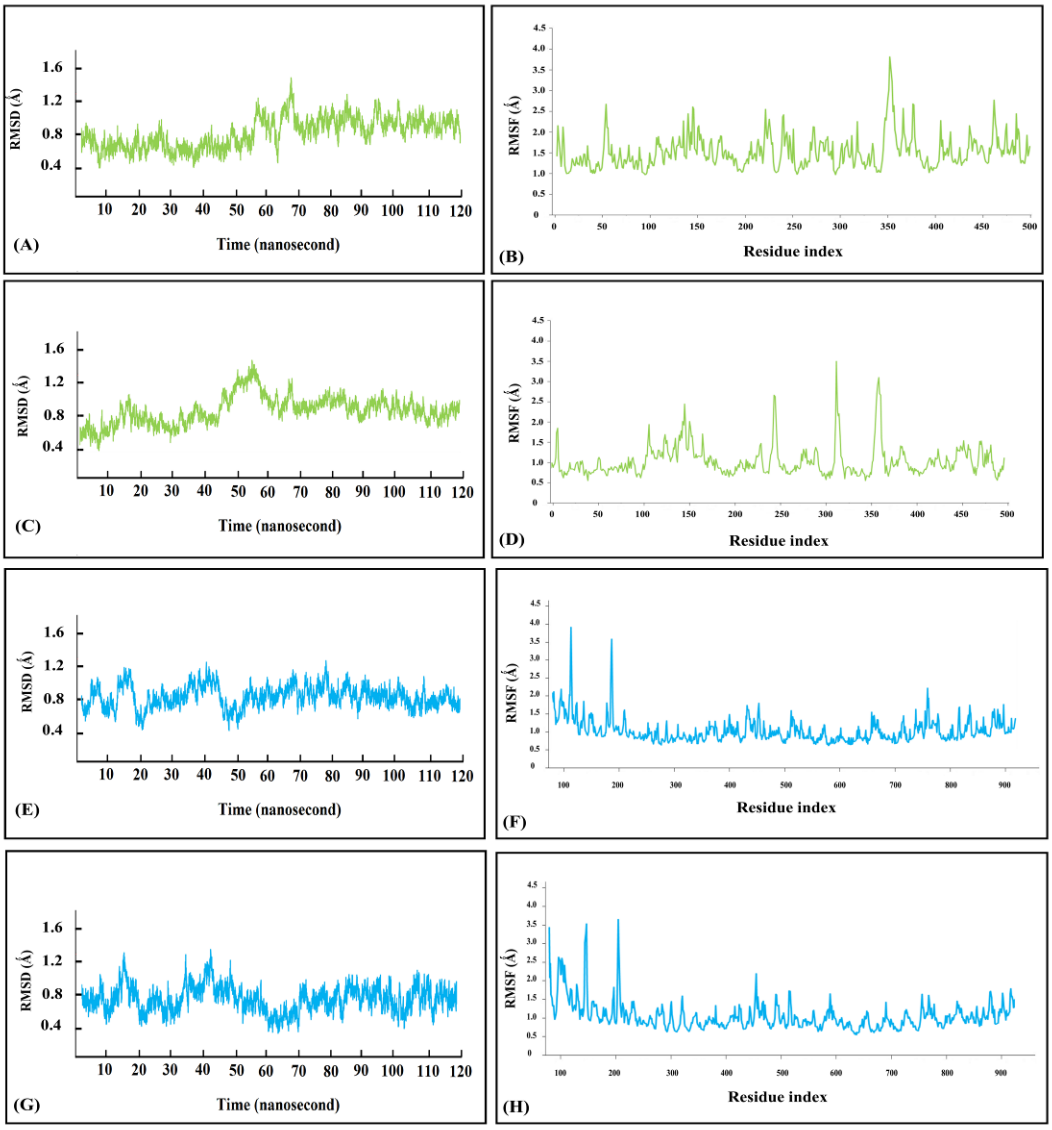


Figure 7. (A) RMSD analysis of the complex stigmasterol - α-amylase protein. **(B)** RMSF analysis of the complex stigmasterol - α-amylase protein. **(C)** RMSD analysis of the complex β-sitosterol - α-amylase protein. **(D)** RMSF analysis of the complex β-sitosterol - α-amylase protein. **(E)** RMSD analysis of the complex stigmasterol - α- glucosidase protein. **(F)** RMSF analysis of the complex stigmasterol - α- glucosidase protein. **(G)** RMSD analysis of the complex β-sitosterol - α- glucosidase protein. **(F)** RMSF analysis of the complex β-sitosterol - α- glucosidase protein.

(complex 3), and β-sitosterol-α-glucosidase (complex 4) were 2.1, 1.4, 1.1, and 0.88 Å, respectively. Muralidharan et al. (2020) have observed that the residues that undergo significant variations during MD simulations are represented by peaks in the RMSF plot. It was evident that complexes 1, 2, 3, and 4's RMSF analysis displayed the fewest changes and remained largely constant during the 120 ns MD simulations, demonstrating the complexes' conformation stability (Fig. 7B, D, F, and H). If a complex's interaction patterns do not significantly change between the pre- and post-MD simulations, then the protein-ligand complex is thought to be stable in its conformation (Khan et al., 2020). After running MD simulations for 120 ns, a thorough examination of the complexes' interaction profiles showed that their binding patterns remained unchanged. Thus, it was clear that the complexes backed up the earlier findings of the molecular docking experiments and were conformationally stable.

CONCLUSION

Based on extensive molecular docking, drug-likeness features, and MD simulations studies, the current research suggests that previously identified bioactive compounds in *Cyperus sexangularis* leaf extract, including stigmasterol and β-sitosterol were the best-scoring lead compounds with remarkable inhibi-

tory properties against the digestive enzymes, α-amylase and α-glucosidase, *in silico*. However, sufficient *in vivo* and mechanistic studies are required to fully establish the anti-hyperglycemic effects of *C. sexangularis* extracts and their putative compounds, particularly stigmasterol and β-sitosterol.

CONFLICT OF INTEREST

The authors declare no conflicts of interest.

ACKNOWLEDGMENTS

The authors acknowledge the support of the National Research Foundation (NRF) South Africa through the NRF rated incentive grant. The Directorate of Research Development and Innovation and the African Medicinal Flora and Fauna Research Niche, Walter Sisulu University, South Africa, are also acknowledged for funding support. The authors also acknowledge Prof. Namrita Lall, University of Pretoria, and the Water Research Commission, South Africa.

REFERENCES

Abraham MJ, Murtola T, Schulz R, Páll S, Smith JC, Hess B, Lindahl E (2015) GROMACS: High performance molecular simulations through multi-level parallelism from laptops to supercomputers. SoftwareX 1: 19–25. https://doi.org/10.1016/j.softx.2015.06.001

Ames BN, Durston WE, Yamasaki E, Lee FD (1973) Carcinogens are mutagens: a simple test system combining liver homogenates for activation and bacteria for detection. Proc Natl Acad Sci USA 70(8): 2281–2285. https://doi.org/10.1073/pnas.70.8.2281

Assefa ST, Yang EY, Chae SY, Song M, Lee J, Cho MC, Jang S (2019) Alpha glucosidase inhibitory activities of plants with focus on common vegetables. Plants 9(1): 2. https://doi.org/10.3390/plants9010002

Baell JB (2010) Observations on screening-based research and some concerning trends in the literature. Future Med Chem 2(10): 1529–1546. https://doi.org/10.4155/fmc.10.237

Banerjee P, Eckert AO, Schrey AK, Preissner R. (2018) ProTox-II: A webserver for the prediction of toxicity of chemicals. Nucleic Acids Res 46(W1): 257–263. https://doi.org/10.1093/nar/gky318

Benigni R, Bossa C (2011) Mechanisms of chemical carcinogenicity and mutagenicity: a review with implications for predicting toxicology. Chem Rev 111(4): 2507–2539. https://doi.org/10.1021/cr100222q

Binkowski TA, Naghibzadeh S, Liang J (2003) CASTp: Computed atlas of surface topography of proteins. Nucleic Acids Res 31(13): 3352–3355. https://doi.org/10.1093/nar/gkg512

Blind E, Janssen H, Dunder K, de Graeff PA (2018) The European medicines agency's approval of new medicines for type 2 diabetes. Diabetes Obes Metab 20(9): 2059–2063. https://doi.org/10.1111/dom.13349

Blomme EA, Will Y (2016) Toxicology strategies for drug discovery: present and future. Chem Res Toxicol 29(4): 473–504. https://doi.org/10.1021/acs.chemrestox.5b00407

Caner S, Brayer GD (2016) Human pancreatic alpha-amylase in complex with mini-montbretin A. Canadian Institutes of Health Research (CIHR). http://dx.doi.org/10.2210/pdb4w93/pdb

Daina A, Michielin O, Zoete V (2017) Swiss ADME: A free web tool to evaluate pharmacokinetics, drug-likeness and medicinal chemistry friendliness of small molecules. Sci Rep 7: 42717. https://doi.org/10.1038/srep42717

Doak BC, Over B, Giordanetto F, Kihlberg J (2014) Oral druggable space beyond the rule of 5: Insights from drugs and clinical candidates. Chem Biol 21(9): 1115–1142. https://doi.org/10.1016/j.chembiol.2014.08.013

Egan WJ, Merz KM, Baldwin JJ (2000) Prediction of drug absorption using multivariate statistics. J Med Chem 43(21): 3867–3877. https://doi.org/10.1021/jm000292e

Elfiky AA, Azzam EB (2020) Novel guanosine derivatives against MERS CoV polymerase: An in silico perspective. J Biomol Struct Dyn 39(8): 2923–2931. https://doi.org/10.1080/07391102.2020.1758789

Enayatkhani M, Hasaniazad M, Faezi S, Guklani H, Davoodian P, Ahmadi N, Ahmadi K (2020) Reverse vaccinology approach to design a novel multi-epitope vaccine candidate against COVID-19: An in silico study. J Biomol Struct Dyn 39(8): 2857–2872. https://doi.org/10.1080/07391102.2020.1756411

Gentile D, Patamia V, Scala A, Sciortino MT, Piperno A, Rescifina A (2020) Putative inhibitors of SARS-CoV-2 main protease from a library of marine natural products: a virtual screening and molecular modeling study. Mar Drugs 18(4): 225. https://doi.org/10.3390/md18040225

Gleeson MP, Hersey A, Hannongbua S (2011) *In-silico* ADME models: a general assessment of their utility in drug discovery and applications. Curr Top Med Chem 11(4): 358–381. https://doi.org/10.2174/156802611794480927

Gothai S, Ganesan P, Park SY, Fakurazi S, Choi DK, Arulselvan P (2016) Natural phyto-bioactive compounds for the treatment of type 2 diabetes: Inflammation as a target. Nutrients 8(8): 461. https://doi.org/10.3390/nu8080461

Harborne JB (1998) Phytochemical methods: A Guide to Modern Techniques of Plant Analysis. 3rd ed. Springer Dordrecht, 302 pp.

IDF (2016) IDF Diabetes Atlas, (7 editions), IDF, Brussels, Belgium.

Joshi AJ, Gadhwal MK, Joshi UJ (2014) A combined approach based on 3D pharmacophore and docking for identification of new aurora A kinase inhibitors. Med Chem Res 23: 1414–1436. https://doi.org/10.1007/s00044-013-0747-5

Kar P, Kumar V, Vellingiri B, Sen A, Jaishee N, Anandraj A, Malhotra H, Bhattacharyya S, Mukhopadhyay S, Kinoshita M, Govindasamy V, Roy A, Naidoo D, Subramaniam MD (2022a) Anisotine and amarogentin as promising inhibitory candidates against SARS-CoV-2 proteins: A computational investigation. J Biomol Struct Dyn 40(10): 4532–4542. https://doi.org/10.1080/07391102.2020.1860133

Kar P, Sharma NR, Singh B, Sen A, Roy A (2021) Natural compounds from *Clerodendrum* spp. as possible therapeutic candidates against SARS-CoV-2: An *in silico* investigation. J Biomol Struct Dyn 39(13): 4774–4785. https://doi.org/10.1080/07391102.2020.1780947

Kar P. Saleh-E-In MM, Jaishee N, Anandraj A, Kormuth E, Vellingiri B, Angione C, Rahman PKSM, Pillay S, Sen A, Naidoo D, Roy A, Choi YE (2022b) Computational profiling of natural compounds as promising inhibitors against the spike proteins of SARS-CoV-2 wild-type and the variants of concern, viral cell-entry process, and cytokine storm in COVID-19. J Cell Biochem 123(5): 964–986. https://doi.org/10.1002/jcb.30243

Kaur N, Kumar V, Nayak SK, Wadhwa P, Kaur P, Sahu SK (2021) Alpha-amylase as a molecular target for treatment of diabetes mellitus: A comprehensive review. Chem Biol Drug Des 98(4): 539–560. https://doi.org/10.1111/cbdd.13909

Khan SA, Zia K, Ashraf S, Uddin R, Ul-Haq Z (2020) Identification of chymotrypsin-like protease inhibitors of SARS-CoV-2 *via* integrated computational approach. J Biomol Struct Dyn 39(7): 2607–2616. https://doi.org/10.1080/07391102.2020.1751298

Kroes R, Renwick AG, Cheeseman M, Kleiner J, Mangelsdorf I, Piersma A, Schilter B, Schlatter J, van Schithorst F, Vos JG, Wurtzen G (2004) Structure-based thresholds of toxicological concern (TTC): Guidance for application to substances present at low levels in the diet. Food Chem Toxicol 42(1): 65–83. https://doi.org/10.1016/j.fct.2003.08.006

Lagorce D, Bouslama L, Becot J, Miteva MA, Villoutreix BO (2017) FAF-Drugs4: Free ADME-tox filtering computations for chemical biology and early stages drug discovery. Bioinformatics 33(22): 3658–3660. https://doi.org/10.1093/bioinformatics/btx491

Le MT, Trinh DT, Ngo TD, Tran-Nguyen VK, Nguyen DN, Hoang T, Nguyen HM, Do TG, Mai TT, Tran TD, Thai KM (2022) Chalcone derivatives as potential inhibitors of P-glycoprotein and NorA: an *in silico* and *in vitro* study. Biomed Res Int 2022: 9982453. https://doi.org/10.1155/2022/9982453

Lipinski CA, Lombardo F, Dominy BW, Feeney PJ (2001) Experimental and computational approaches to estimate solubility and permeability in drug discovery and development settings. Adv Drug Deliv Rev 46(1–3): 3–26. https://doi.org/10.1016/s0169-409x(00)00129-0

Manigandan G, Subramaniyan V (2021) Anti-diabetic activities of isolated compound beta-sitosterol from the ethanolic extract of stem of *Andrographis echioides*. Int J Pharm Sci Res 12(9): 5125–5133. https://doi.org/10.13040/IJPSR.0975-8232.12(9).5125-33

Miya GM, Oriola AO, Payne B, Cuyler M, Lall N, Oyedeji AO (2023) Steroids and fatty acid esters from *Cyperus sexangularis* leaf and their antioxidant, anti-inflammatory and anti-elastase properties. Molecules 28(8): 3434. https://doi.org/10.3390/molecules28083434

Muralidharan N, Sakthivel R, Velmurugan D, Gromiha MM (2020) Computational studies of drug repurposing and synergism of lopinavir, oseltamivir and ritonavir binding with SARS-CoV-2 protease against COVID-19. J Biomol Struct Dyn 39(7): 2673–2678. https://doi.org/10.1080/07391102.2020.1752802

Naidoo D, Roy A, Kar P, Mutanda T, Anandraj A (2020) Cyanobacterial metabolites as promising drug leads against the M^{pro} and PL^{pro} of SARS-CoV-2: An *in silico* analysis. J Biomol Struct Dyn 39(16): 6218–6230. https://doi.org/10.1080/07391102.2020.1794972

O'Boyle NM, Banck M, James CA, Morley C, Vandermeersch T, Hutchison GR (2011) Open Babel: An open chemical toolbox. J Cheminf 3: 33. https://doi.org/10.1186/1758-2946-3-33

Petit C, Bujard A, Skalicka-Woźniak K, Cretton S, Houriet J, Christen P, Carrupt PA, Wolfender JL (2016) Prediction of the passive intestinal absorption of medicinal plant extract constituents with the parallel artificial membrane permeability assay (PAMPA). Planta Med 82(5): 424–431. https://doi.org/10.1055/s-0042-101247

Pires DE, Blundell TL, Ascher DB (2015) pkCSM: predicting small-molecule pharmacokinetic and toxicity properties using graph-based signatures. J Med Chem 58(9): 4066–4072. https://doi.org/10.1021/acs.jmedchem.5b00104

Pouliot M, Jeanmart S (2016) Pan assay interference compounds (PAINS) and other promiscuous compounds in antifungal research. J Med Chem 59(2): 497–503. https://doi.org/10.1021/acs.jmedchem.5b00361

Poulose N, Sajayan A, Ravindran A, Chandran A, Priyadharshini GB, Selvin J, Kiran GS (2021) Anti-diabetic potential of a stigmasterol from the seaweed *Gelidium spinosum* and its application in the formulation of nanoemulsion conjugate for the development of functional biscuits. Front Nutr 8: 694362. https://doi.org/10.3389/fnut.2021.694362

Raimondo D, Staden LV, Foden W, Victor JE, Helme NA, Turner RC, Kamundi DA, Manyama PA (2009) Red list of South African plants 2009. South African National Biodiversity Institute.

Raut NA, Gaikwad NJ (2006) Antidiabetic activity of hydro-ethanolic extract of *Cyperus rotundus* in alloxan induced diabetes in rats. Fitoterapia 77(7–8): 585–588. https://doi.org/10.1016/j.fitote.2006.09.006

Roig-Zamboni V, Cobucci-Ponzano B, Iacono R, Ferrara MC, Germany S, Bourne Y, Parenti G, Moracci M, Sulzenbacher G (2017) Structure of human lysosomal acid α-glucosidase–a guide for the treatment of Pompe disease. Nat Commun 8: 1111. https://doi.org/10.1038/s41467-017-01263-3

Saleh-E-In MM, Roy A, Al-Mansur MA, Mahmood Hasan C, Rahim MM, Sultana N, Ahmed S, Islam MR, van Staden J (2019) Isolation and *in silico* prediction of potential drug-like compounds from *Anethum sowa* L. root extracts targeted towards cancer therapy. Comput Biol Chem 78: 242–259. https://doi.org/10.1016/j.compbiolchem.2018.11.025

Salentin S, Schreiber S, Haupt VJ, Adasme MF, Schroeder M (2015) PLIP: fully automated protein-ligand interaction profiler. Nucleic Acids Res 43(W1): 443–447. https://doi.org/10.1093/nar/gkv315

Schüttelkopf AW, Van Aalten DM (2004) PRODRG: A tool for high throughput crystallography of protein-ligand complexes. Acta Crystallogr D Biol Crystallogr 60(8): 1355–1363. https://doi.org/10.1107/S0907444904011679

Schyman P, Liu R, Desai V, Wallqvist A (2017) vNN web server for ADMET predictions. Front Pharmacol 8: 889. https://doi.org/10.3389/fphar.2017.00889

Singh P, Khosa RL, Mishra G, Jha KK (2015) Antidiabetic activity of ethanolic extract of *Cyperus rotundus* rhizomes in streptozotocin-induced diabetic mice. J Pharm Bioallied Sci 7(4): 289–292. https://doi.org/10.4103/0975-7406.168028

Todd JA (2010) Etiology of type 1 diabetes. Immunity 32(4): 457–467. https://doi.org/10.1016/j.immuni.2010.04.001

Umesh Kundu D, Selvaraj C, Singh SK, Dubey VK (2020) Identification of new anti-nCoV drug chemical compounds from Indian spices exploiting SARS-CoV-2 main protease as target. J Biomol Struct Dyn 39(9): 3428–3434. https://doi.org/10.1080/07391102.2020.1763202

Veber DF, Johnson SR, Cheng HY, Smith BR, Ward KW, Kopple KD (2002) Molecular properties that influence the oral bioavailability of drug candidates. J Med Chem 45(12): 2615–2623. https://doi.org/10.1021/jm020017n

Wang YY, Li J, Wu ZR, Zhang B, Yang HB, Wang Q, Cai, YC, Liu GX, Li WH, Tang Y (2017) Insights into the molecular mechanisms of *Polygonum multiflorum* Thunb-induced liver injury: A computational systems toxicology approach. Acta Pharmacol Sin 38(5): 719–732. https://doi.org/10.1038/aps.2016.147

Waring MJ, Arrowsmith J, Leach AR, Leeson PD, Mandress S, Owen RM, Pairaudeau G, Pennie WD, Pickett WD, Wang J, Wallace O, Weir A (2015) An analysis of the attrition of the drug candidates from four major pharmaceutical companies. Nat Rev Drug Discov 14: 475–486. https://doi.org/10.1038/nrd4609

Yang H, Lou C, Sun L, Li J, Cai Y, Wang Z, Li W, Liu G, Tang Y (2019) admetSAR 2.0: Web-service for prediction and optimization of chemical ADMET properties. Bioinformatics 35(6): 1067–1069. https://doi.org/10.1093/bioinformatics/bty707

Yanuar A, Pratiwi I, Syahdi RR (2018) *In silico* activity analysis of saponins and 2, 5-piperazinedione from marine organism against murine double minute-2 inhibitor and procaspase-3

activator. J Young Pharm 10(2s): S16–S19. https://doi.org/10.5530/jyp.2018.2s.4

Yerlikaya PO, Arisan ED, Mehdizadehtapeh L, Uysal-Onganer P, Gürkan A (2023) The use of plant steroids in viral disease treatments: current status and future perspectives. Eur J Biol 82(1): 86-94. https://doi.org/10.26650/EurJBiol.2023.1130357

AUTHOR CONTRIBUTION:

Contribution	Miya GM	Kar P	Oriola AO	Oyedeji AO
Concepts or ideas	x	x	x	x
Design		x	x	x
Definition of intellectual content		x	x	
Literature search		x	x	
Experimental studies		x	x	
Data acquisition	x	x	x	
Data analysis		x	x	
Statistical analysis		x	x	
Manuscript preparation	x	x	x	
Manuscript editing		x	x	
Manuscript review	x	x	x	x

Citation Format: Miya GM, Kar P, Oriola AO, Oyedeji AO (2025) Antidiabetic potential of isolated compounds from *Cyperus sexangularis* Nees: An *in silico* molecular docking and dynamic-based approach. J Pharm Pharmacogn Res 13(2): 647–661. https://doi.org/10.56499/jppres24.2050_13.2.647

Publisher's Note: All claims expressed in this article are solely those of the authors and do not necessarily represent those of their affiliated organizations, or those of the publisher, the editors and the reviewers. Any product that may be evaluated in this article, or claim that may be made by its manufacturer, is not guaranteed or endorsed by the publisher.

Open Access: This article is distributed under the terms of the Creative Commons Attribution 4.0 International License (http://creativecommons.org/ licenses/by/4.0/), which permits use, duplication, adaptation, distribution and reproduction in any medium or format, as long as you give appropriate credit to the original author(s) and the source, provide a link to the Creative Commons license and indicate if changes were made.